

## Trend Quality Ozone from NPP OMPS: the Version 2 Processing

Richard McPeters<sup>1</sup>, Stacey Frith<sup>2</sup>, Natalya Kramarova<sup>1</sup>, Jerry Ziemke<sup>3</sup>, and Gordon Labow<sup>2</sup>

**Abstract.** A version 2 processing of data from two ozone monitoring instruments on Suomi NPP, the OMPS nadir ozone mapper and the OMPS nadir ozone profiler, has now been completed. The previously released data were useful for many purposes but were not suitable for use in ozone trend analysis. In this processing, instrument artifacts have been identified and corrected, an improved scattered light correction and wavelength registration have been applied, and soft calibration techniques were implemented to produce a calibration consistent with data from the series of SBUV/2 instruments. The result is a high quality ozone time series suitable for trend analysis. Total column ozone data from the OMPS nadir mapper now agree with data from the SBUV/2 instrument on NOAA 19 with a zonal average bias of -0.2% over the 60°S to 60°N latitude zone. Differences are somewhat larger between OMPS nadir profiler and N19 total column ozone, with an average difference of -1.1 % over the 60°S to 60°N latitude zone and a residual seasonal variation of about 2% at latitudes higher than about 50 degrees. For the profile retrieval, zonal average ozone in the upper stratosphere (between 2.5 and 4 hPa) agrees with that from NOAA 19 within ±3% and an average bias of -1.1%. In the lower stratosphere (between 25 and 40 hPa) agreement is within ±3% with an average bias of +1.1%. Tropospheric ozone produced by subtracting stratospheric ozone measured by the OMPS limb profiler from total column ozone measured by the nadir mapper is consistent with tropospheric ozone produced by subtracting stratospheric ozone from MLS from total ozone from the OMI instrument on Aura. The agreement of tropospheric ozone is within 10% in most locations.

<sup>1</sup>NASA Goddard Space Flight Center, Greenbelt Maryland

<sup>2</sup>Science Systems and Applications Inc., Lanham, Maryland

<sup>3</sup>Morgan State University, Baltimore. Maryland

35 **1. Introduction**

36  
37 NASA has been measuring ozone from space since the launch of the Backscatter  
38 Ultraviolet (BUV) instrument on Nimbus 4 in 1970. The series of follow-on instruments, SBUV  
39 (Solar Backscatter Ultraviolet) and TOMS (Total Ozone Mapping Spectrometer) on Nimbus 7  
40 and SBUV/2 instruments on NOAA 9, 11, 14, 16, 17, 18, and 19 produced a long term time  
41 series of global ozone observations. Under NASA's MEASUREs (Making Earth System data  
42 records for Use in Research Environments) program, data from this series of instruments were  
43 re-processed to create a coherent ozone time series. Inter-instrument comparisons during periods  
44 of overlap as well as comparisons with data from other satellite and ground based instruments  
45 were used to evaluate the consistency of the record and make careful calibration adjustments as  
46 needed (McPeters et al., 2013). The result is an ozone data record suitable for trend studies that  
47 we designated the Merged Ozone Data (MOD) time series (Frith et al., 2014). Ozone instruments  
48 on the Suomi-NPP spacecraft and the planned series of JPSS (Joint Polar Satellite System)  
49 spacecraft will now be used to continue this series of measurements in order to document long-  
50 term ozone change.

51 The Suomi National Polar-orbiting Partnership (Suomi NPP) is a joint NOAA/NASA  
52 mission that collects and distributes remotely sensed land, ocean, and atmospheric data to the  
53 meteorological and global climate change communities. Suomi NPP was launched October 28,  
54 2011. The Ozone Mapper Profiler Suite (OMPS) on NPP consists of three instruments - the  
55 ozone total column Nadir Mapper (NM), an instrument similar to the TOMS and OMI ozone  
56 mapping instruments, the Nadir Profiler (NP), an instrument similar to the SBUV and SBUV/2  
57 profilers, and the Limb Profiler (LP), an instrument that measures the ozone vertical distribution  
58 using light scattered from the Earth's limb. Details of the OMPS instruments and mission are  
59 given by Flynn et al. (2006).

60 The purpose of the version 2 processing of data from the two OMPS nadir sensors, which is  
61 the subject of this paper, is to correct various instrument artifacts and to apply an updated  
62 calibration that will be consistent with data from earlier instruments. Only the reprocessed  
63 version 2 data from the two nadir instruments will be discussed here. While some comparisons  
64 with data from the Limb Profiler will be shown in this paper, detailed LP validation results will  
65 be discussed in other papers.

66  
67 **2. The OMPS Nadir Mapper and Nadir Profiler**

68  
69 The OMPS nadir mapper (NM) is a nadir viewing, wide swath, ultraviolet-visible imaging  
70 spectrometer that provides daily global measurements of the solar radiation backscattered by the  
71 Earth's atmosphere and surface, along with measurements of the solar irradiance. It shares a  
72 telescope with the OMPS nadir profiler (NP) spectrometer. A dichroic filter splits light from the  
73 telescope into two streams. Most of the 310-380 nm light is transmitted to the NM instrument,  
74 while most of the 250-300 nm light is reflected to the NP instrument. The transition between  
75 reflection and transmission occurs between 300 and 310 nm, the wavelength overlap region. The

76 detector for each instrument is a 340x740 pixel CCD (Charge Coupled Device). For more details  
77 on the instruments and sensors see Seftor et al. (2013).

78 Unlike the heritage TOMS instruments which measured ozone using a photomultiplier  
79 detector at six discrete wavelengths (from 306 to 380 nm, depending on the instrument), the NM  
80 instrument measures the complete spectrum from 300 to 380 nm at an average spectral resolution  
81 of 1.1 nm. The OMPS-NM sensor has a 110 degree cross-track field of view, with 35 discrete  
82 cross-track bins. The 0.27  $\mu\text{m}$  along track slit width produces a 50 km spatial resolution near  
83 nadir. An algorithm (Bhartia, 2007) uses the radiance and irradiance measurements to infer total  
84 column ozone. As illustrated in Figure 1, the OMPS NM makes 400 individual scans per orbit  
85 with 35 across-track measurements in each scan, which provides full global coverage of the  
86 sunlit Earth every day. Resolution of a single FOV at nadir is 50 km by 50 km, while the full  
87 swath width covers approximately 2000 km.

88 The OMPS nadir profiler (NP) has a 16.6  $\mu\text{m}$  cross-track slit and a 0.26  $\mu\text{m}$  along-track slit  
89 width, producing a ground FOV cell size of 250 km by 250 km when exposed for a 38 second  
90 sample time. The OMPS NP instrument makes 80 measurements per orbit, resulting in full  
91 global coverage approximately every 6 days. The NP measures the complete spectrum from 250  
92 to 310 nm with a 1.1 nm bandpass. Because the NP itself only makes measurements up to a  
93 maximum wavelength of 310 nm, the longer wavelengths that are needed in the retrievals at high  
94 latitudes must be taken by averaging the overlap cells from the NM instrument, the 5 central  
95 cross track cells in 5 along track scans.

### 96 97 **3. The Version 2 Processing**

99 The goal of the version 2 processing is to produce ozone data sufficiently accurate to be  
100 used to continue the Merged Ozone Data (MOD) time series. This time series is a unified multi-  
101 instrument ozone data set created by merging data from a series of SBUV and SBUV/2  
102 instruments beginning with the original BUV instrument launched on Nimbus 4 in 1970 and  
103 extending to the SBUV/2 instrument on NOAA 19, which continues to operate. Data from these  
104 instruments were recently reprocessed as version 8.6 with a consistent calibration to create a  
105 coherent ozone time series (McPeters et al., 2013). The MOD data set created from this series is  
106 described in detail by Frith et al. (2014). Figure 2 shows the MOD fit to data from three recent  
107 SBUV/2 instruments, on NOAA 16, 18, and 19, for which good data are available during the  
108 OMPS observation period. Comparison with ozone from ground networks shows that total ozone  
109 in the MOD series is consistent to within about a percent for the recent data. Data from the  
110 OMPS NP and NM instruments will be used to extend this MOD data record.

111 In the version 2 processing we use the latest version of the Level 1 data, the dataset of  
112 calibrated radiance measurements from NM and NP that implements a refined calibration for  
113 both instruments (Seftor et al., 2014) and corrects for several instrument effects. Both the NM  
114 and NP L1b data now use an improved set of calibration coefficients that exhibit smoother  
115 wavelength-to-wavelength behavior and provide a wavelength registration that accounts for  
116 intra-orbital (for the NM) and intra-seasonal (for the NP) shifts that were identified in analysis of  
117 the data. A small bandpass error in the NP instrument near 295 nm was corrected, and errors in

118 the pre-launch calibration measurements in the dichroic transition region (300 - 310 nm) for both  
119 instruments were identified and corrected. The daily dark current correction has been refined for  
120 each instrument.

121 Soft (in orbit) calibration techniques were used to refine the instrument calibration. The  
122 NM pre-launch calibration of the 331 nm channel, which is used to determine reflectivity, was  
123 not adjusted at nadir since the measured radiance over ice matched the expected radiance  
124 (determined from other instruments such as Earth Probe TOMS and OMI) to within 1%. Cross-  
125 track adjustments to this channel to "flatten" the 331 nm reflectivity calculation over ice were  
126 then determined and applied. Similarly, the nadir radiance at 317 nm, which is the channel used  
127 to determine ozone, was not changed; the off-nadir radiances were then adjusted to take out any  
128 cross track ozone dependence. The 317 and 331 nm NM nadir radiances are also used in the NP  
129 algorithm retrieval, with no adjustments applied. For the NM radiances at 312 nm, which are  
130 used in the NP algorithm but not in the NM algorithm, an adjustment was determined, and  
131 applied to minimize the final retrieval residuals. Similarly, the NP 306 nm radiances were  
132 adjusted to minimize the final residuals. The calibrations were not explicitly adjusted to agree  
133 with the NOAA 19 SBUV/2 calibration, so NOAA 19 comparisons can be used for validation.

134 The algorithm used to retrieve total column ozone from the NM is very similar to the v8.5  
135 algorithm used in the processing of data from Aura OMI instrument as described by Bhartia  
136 (2007), and Bhartia et al. (2004). The basic algorithm uses two wavelengths to derive total  
137 column ozone, one wavelength with weak ozone absorption (331 nm) to characterize the  
138 underlying surface and clouds, and the other at a wavelength with strong ozone absorption (317  
139 nm). The ozone retrieval algorithms for both the NP and NM instruments now use the Brion/  
140 Daumont / Malicet ozone cross sections (Brion et al., 1993) to be consistent with other data sets  
141 in the MOD time series.

142 The NP retrieval algorithm uses 12 discrete wavelengths to retrieve ozone profiles  
143 employing Rodgers' optimal estimation technique (Bhartia et al., 2013). It is very similar to the  
144 v8.6 algorithm used to reprocess the SBUV and SBUV/2 data sets (McPeters et al., 2013) used in  
145 the MOD time series. While the vertical resolution of an OMPS NP ozone retrieval is somewhat  
146 coarse in comparison with the LP sensor, about 8 km resolution in the stratosphere, NP provides  
147 valuable data for the continuation of the historical SBUV/2 ozone data record, and for validation  
148 of the OMPS LP retrievals.

#### 149 **4. Total Column Ozone Comparisons**

150  
151  
152 The accuracy and stability of the OMPS ozone data record has been evaluated through  
153 comparisons with ground-based observations and comparisons with other satellite data sets. The  
154 worldwide network of Dobson and Brewer stations has been used for years for ground-based  
155 validation of total column ozone. For satellite validation of total ozone, comparisons with the  
156 MOD data set are used as a primary standard for this evaluation. Validation of profile ozone (in  
157 section 5) will use data from balloon sondes, data from the currently operating SBUV/2  
158 instrument on NOAA 19, and data from the microwave limb sounder (MLS) on the Aura  
159 spacecraft.

160 Figure 3 compares average ozone from 52 ground based Brewer and Dobson stations in the  
161 northern hemisphere with coincident observations of ozone measured by the NM instrument over  
162 the individual stations (Labow et al., 2013). Comparison with ozone from the NOAA 19  
163 SBUV/2 is also shown (in blue) since these data are the basis of much of the NM and NP  
164 validation. Northern hemisphere comparisons are shown because the network density is much  
165 better in the northern hemisphere than in the southern, and comparisons in a single hemisphere  
166 will illuminate any seasonally dependent errors. Such comparisons have been shown capable of  
167 detecting instrument changes over the long term of a few tenths of a percent (McPeters et al.,  
168 2008). The comparison covers the period from April 2012 through the end of 2016. Figure 3  
169 shows that the agreement of NM total ozone is mostly within half a percent. The linear fit in  
170 Figure 3 shows that OMPS NM has very little drift in ozone relative to the ground observations,  
171 (0.8% per decade) and an average bias of less than 0.2%.

172 The comparison of ozone from the NM instrument with ozone from the MOD (merged  
173 ozone dataset) time series shown in Figure 4 illustrates the improved accuracy of the version 2  
174 processing. The monthly zonal average ozone, area weighted for the latitude zone from 60°S to  
175 60°N, is plotted. Because ozone is derived from measurements of backscattered sunlight, data are  
176 not always available in winter months at latitudes above 60 degrees. MOD ozone for this time  
177 period is based on combining ozone from SBUV/2 instruments on three satellites, NOAA 16, 18,  
178 and 19. For the period from March 2014 to 2017 only the instrument on NOAA 19 was  
179 operational. The lower panel in Figure 4 shows the NM monthly average ozone for the old  
180 version 1 processing (dashed red curve) and the new version 2 processing (solid blue curve)  
181 along with MOD average ozone (orange curve). The upper panel shows the percent difference of  
182 version 1 and version 2 ozone from MOD ozone. Where in version 1 NM ozone was on average  
183 1% high relative to MOD, in the version 2 processing it is 0.2% low. There is a small relative  
184 trend between NM and MOD of 0.8% per decade. This relative trend could be due to either NM  
185 or to an aging NOAA 19 SBUV/2 instrument in a drifting orbit. Further comparisons will be  
186 needed to distinguish between the two possibilities.

187 Figure 5 is the same plot but for total column ozone measured by the NP instrument. NP  
188 total column ozone is derived by integrating the retrieved ozone profiles. In principle, this should  
189 be more accurate over a broad range of solar zenith angles than ozone derived from the limited  
190 wavelength range of the NM instrument. Here the average relative bias of about +1.4% in  
191 version 1 is reduced to -1.05% in version 2. This bias disagreement between NM and NP means  
192 that there is a small inconsistency between the two instruments that has not been resolved. This  
193 issue of the relative calibration inconsistency is being studied. There is a relative drift of NP  
194 ozone relative to MOD that is similar to that for the NM instrument, of 0.5% per decade. To the  
195 extent that the NP and NM instruments have independent calibrations, this suggests that the  
196 small relative drift is due to the NOAA 19 SBUV/2 instrument calibration and the effect of the  
197 drifting orbit.

198 Figure 6 shows the latitude dependence relative to MOD of the version 2 ozone from the  
199 mapper and from the profiler. The lower panel plots ozone averaged for five Marches from 2013  
200 through 2016, while the upper panel shows the percent difference from MOD for the same  
201 months. The latitude dependence of ozone varies by season so it is useful to examine individual

202 months, and latitude coverage is maximum near an equinox. The NM instrument has very little  
203 latitude dependence except at the highest southern latitudes where ozone is low. The NP  
204 instrument has the bias as noted in Figure 5 and likewise has little latitude dependence at low to  
205 mid latitudes. The higher ozone (by 2 to 3 percent) for retrievals at latitudes greater than 50° may  
206 be a solar zenith angle dependent manifestation of what is possibly an NP calibration error.

## 207 208 **5. Ozone Profile Comparisons**

209  
210 The long-term behavior of ozone as a function of altitude is in some ways more interesting  
211 than the behavior of total column ozone because it can be used to confirm the accuracy of  
212 various model predictions. However, the accuracy of these measurements is more difficult to  
213 validate (Hassler et al., 2014). Data from the ozone sonde network can be used to validate the  
214 profile in the troposphere and lower stratosphere, while satellite data can be used to validate the  
215 middle to upper stratospheric results. There are ground-based measurements of the ozone vertical  
216 distribution by LIDAR and by microwave sounders, but such measurements are very sparse.  
217 There are umkehr measurements by Dobson and Brewer instruments, but vertical resolution is  
218 coarse and uncertainty is high, especially when aerosols are present.

219 Looking at ground based comparisons of ozone in the lower stratosphere first, Figure 7  
220 compares NP ozone profiles with ozone measured by ECC ozone sondes from one station, Hilo,  
221 Hawaii (20°N, 155°W), a subtropical station with a good time series of sonde launches. The  
222 sonde data are from the SHADOZ network under which the sonde data were reprocessed to  
223 apply the most recent corrections (Witte et al., 2016). For this figure, all 33 of the sondes  
224 launched in 2016 were averaged. The coincident profiles measured by NP were usually within  
225 one degree of latitude and within fifteen degrees of longitude. The comparison shows that in the  
226 lower stratosphere NP agrees with sonde data to within ±5%. Only altitudes between 10 and 50  
227 hPa (approximately 20 to 32 km) are shown because the SBUV nadir ozone retrieval algorithm  
228 produces little profile information on the distribution of ozone below 20 km. But it should be  
229 noted that the column amount of ozone in the troposphere is retrieved accurately (Bhartia et al.,  
230 2013), as evidenced by the fact that total column ozone from an SBUV retrieval is accurate to  
231 one percent or better (McPeters et al., 2013). This accuracy is critical to the derivation of  
232 tropospheric ozone discussed in section 6.

233 For the middle to upper stratosphere, monthly zonal means comparisons with other satellite  
234 observations of the ozone vertical distribution is the best approach for evaluating the accuracy of  
235 the version 2 NP results. Figure 8 shows the time dependent difference of NP from the NOAA 19  
236 SBUV/2 retrievals averaged over low to middle latitudes (40°S to 40°N), for the upper  
237 stratosphere (2.5 - 4 hPa), lower stratosphere (25 - 40 hPa), and total column ozone. Comparing  
238 with N19 only rather than MOD gives a bit more uniformity for the time dependent profile  
239 comparison. In both the upper stratosphere and lower stratosphere the vsn 2 ozone agrees with  
240 the N19 ozone to within about one percent, where in the NP version 1 retrievals, ozone was  
241 higher by 4% and 6% respectively. There is no evidence of a significant time dependent  
242 difference in total ozone, but in the middle stratosphere there appears to be a small increase in  
243 ozone of about 2% over 6 years. There is the bias in total column ozone as noted earlier of a bit

244 over one percent. While the use of NM wavelengths in the NP retrieval may contribute to the  
245 bias, the bigger problem appears to be a wavelength dependent calibration error in the NP itself.  
246 This possibility is being studied.

247 Ozone agreement as a function of altitude is shown in Figure 9 where ozone in low to  
248 middle latitudes is averaged for five Junes from 2012 through 2016. Selecting a single month for  
249 this comparison allows us to see any seasonal effect that might be suppressed in the annual  
250 average. As will be shown later, there are seasonal variations in NP ozone at high latitudes. The  
251 stratospheric ozone mixing ratio is plotted for OMPS NP vsn 2, for NOAA 19 SBUV/2, for the  
252 Aura Microwave Limb Sounder (MLS) (Froidevaux et al., 2008), and for the OMPS limb  
253 profiler (LP). The right panel shows the agreement of the OMPS NP vsn 2 ozone profile with  
254 each of the three other profile measurements by plotting the percent difference from each.  
255 Agreement is almost always within  $\pm 5\%$ , which experience has shown to be fairly good  
256 agreement for profile comparisons. While agreement in the upper stratosphere and lower  
257 stratosphere shown in Figure 8 was good, Figure 9 shows that there is a significant underestimate  
258 of ozone relative to NOAA 19, MLS and LP in the 6 to 10 hPa region. This is likely the source  
259 of much of the disagreement in total column ozone. It has been noted in other comparisons  
260 (*Hassler et al.*, 2014), that NOAA 19 ozone is a bit high in the upper stratosphere relative to  
261 MLS profiles, and a similar result is seen here for the NP retrievals.

262 The NP vsn 2 ozone has somewhat different behavior at low to mid latitudes than at high  
263 latitudes. The ozone anomaly, the percent difference of NP ozone from the NOAA 19 SBUV  
264 ozone, is shown for low to mid latitudes ( $<45^\circ$ ) in Figure 10, and for higher latitudes ( $>45^\circ$ ) in  
265 Figure 11. For each figure the anomaly is shown for total column ozone (lower panel), for lower  
266 stratospheric ozone (layer from 25 hPa to 40 hPa) in the middle panel, and for upper  
267 stratospheric ozone (layer from 2.5 hPa to 4 hPa) in the upper panel. Figure 10 shows that vsn 2  
268 ozone at latitudes below  $45^\circ$  agrees well with N19 ozone, while Figure 11 shows that at latitudes  
269 at  $50^\circ$  and above ozone has a significant seasonal dependence that differs from that of N19 with  
270 about 2 to 4% amplitude. This difference is likely another manifestation of a possible NP  
271 calibration error. While this error is small, we are working to resolve it in order to produce a  
272 better NP ozone product.

## 273 274 **6. Tropospheric Ozone from OMPS**

275  
276 Ziemke et al. (2011, 2014, and references therein) have shown that tropospheric ozone can  
277 be derived by subtracting stratospheric ozone from total column ozone. This technique has most  
278 recently been applied by subtracting stratospheric ozone measured by the Aura MLS instrument  
279 from total column ozone measured by the Aura OMI instrument. The OMI/MLS tropospheric  
280 ozone time series currently spans over 12 years and has been a central data product for each of  
281 the BAMS State of the Climate Reports since 2013 and will be used in the upcoming  
282 international Tropospheric Ozone Assessment Report.

283 The OMPS ozone measurements can also be used to calculate tropospheric ozone and  
284 continue the current OMI/MLS time series of measurements should either of the Aura  
285 instruments fail. Because the OMPS instrument suite includes both a total ozone mapper (NM)

286 and a limb profiler (LP), a similar technique can be applied as with OMI/MLS. Figure 12 shows  
287 the tropospheric ozone time series for two locations in the tropics, Java and Brazil, and two  
288 locations at northern mid-latitudes, Beijing, and Washington DC. In each case the red dashed  
289 curve shows tropospheric ozone derived by subtracting MLS stratospheric ozone from OMI total  
290 column ozone. For comparison, the blue solid curve shows the same tropospheric ozone derived  
291 by subtracting stratospheric ozone from the OMPS LP from total column ozone from the NM.  
292 While there are some small differences the overall agreement is quite good. Data on tropospheric  
293 ozone from the NP plus LP combination can be used to continue the tropospheric ozone time  
294 series.

## 295 **7. Data Availability**

296 NPP OMPS version 2 data will shortly be available online from the Goddard DISC:  
297 <https://disc.gsfc.nasa.gov>. Data for the NM mapper and the NP profiler are currently being  
298 converted to HDF5 format for inclusion in the DISC data archive. The calibrated L1 data are also  
299 available from the Goddard DISC. The OMPS NM ozone data are also available in ascii form  
300 from our online site: <https://acd-ext.gsfc.nasa.gov/anonftp/toms/> in the subdirectory omps\_tc.  
301 Data from the NOAA 19 SBUV/2 can also be found here under subdirectory sbuv. The v8.6  
302 MOD data used as our standard for comparison are available from: [https://acdb-](https://acdb-ext.gsfc.nasa.gov)  
303 [ext.gsfc.nasa.gov](https://acdb-ext.gsfc.nasa.gov), then click on “Data\_services” and then on “Merged ozone data”.

## 304 **8. Conclusions**

305 The OMPS nadir mapper (NM) has proven to be a very stable instrument. Comparison with  
306 a network of 52 Northern Hemisphere ground based Dobson and Brewer instruments shows very  
307 good agreement over the four years of operation, agreeing within  $\pm 0.5\%$  with near zero trend.  
308 Total column ozone from the OMPS nadir mapper agrees with MOD ozone and with NOAA 19  
309 SBUV/2 ozone with a bias of  $-0.2\%$  and a small time-dependent drift of  $0.8\%$  per decade. It is  
310 possible that this time dependence could be due to the aging NOAA 19 instrument and its  
311 drifting orbit.

312 The nadir profiler (NP) has likewise been very stable. NP total column ozone has a time  
313 dependence of only  $0.5\%$  per decade relative to MOD or NOAA 19. The bias of  $-1.1\%$  ( $60^\circ\text{S}$  -  
314  $60^\circ\text{N}$ ) is small but inconsistent with ozone from NM. This bias seems to be generated in part by  
315 the negative bias in the 6-10 hPa region. The calibration of the NP instrument near 300 nm is  
316 being examined to understand this inconsistency. NP ozone in the upper stratosphere (2.5 - 4  
317 hPa) and in the lower stratosphere (25 - 40 hPa) agrees well with ozone from NOAA 19 profiler,  
318 with an average difference of  $-1.1\%$  and  $+1.1\%$  respectively at latitudes below  $50^\circ$ . The  
319 retrievals for higher latitudes exhibit a strong seasonal variation of about  $\pm 2\%$ , both in layer  
320 ozone and in total column ozone.

321 Ozone data from these instruments can now be considered “trend quality,” usable to extend  
322 the data record from previous instruments to create an accurate time series. Data from NP at  
323 latitudes above  $50^\circ$  appears to be stable but must be used with a bit of caution because of its  
324



328 residual seasonal variation and because the bias, while small, can be different than at lower  
329 latitudes.

330

331

332 **Acknowledgments**

333 The OMPS nadir profiler and nadir mapper were built by Ball Brothers for flight on the joint  
334 NASA / NOAA NPP satellite. We thank the many people who have worked over the years to  
335 understand the behavior of the OMPS instrument. The Ozone Processing Team has carefully  
336 maintained the calibration of the nadir instruments through both hard and soft calibration  
337 techniques.

338

339 **References**

340

- 341 Bhartia, P.K., Wellemeyer, C. G., Taylor, S., Nath, N., and Gopalan, A., Solar backscatter  
342 ultraviolet (SBUV) version 8 profile algorithm, in Proceedings of the Quadrennial Ozone  
343 Symposium, Kos, Greece, 1-8 June 2004, 295-296, 2004.
- 344 Bhartia, P. K.: Total ozone from backscattered ultraviolet measurements, in: Observing Systems  
345 20 for Atmospheric Composition, L'Aquila, Italy, 20-24 September, 2004, edited by:  
346 Visconti, G., Di Carlo, P., Brune, W., Schoeberl, W., and Wahner, A., Springer, 48–63,  
347 2007.
- 348 Bhartia, P. K., McPeters, R. D., Flynn, L. E., Taylor, S., Kramarova, N. A., Frith, S., Fisher, B.,  
349 and DeLand, M.: Solar Backscatter UV (SBUV) total ozone and profile algorithm, *Atmos.*  
350 *Meas. Tech.*, 6, 2533–2548, doi:10.5194/amt-6-2533-2013, 2013.
- 351 Brion, J., Chakir, A., Daumont, D., Malicet, J., and Parisse, C.: High resolution laboratory  
352 absorption cross section of O<sub>3</sub> temperature effect, *Chem. Phys. Lett.*, 213, 610–612, 1993.
- 353 Flynn, L. E., Seftor, C. J., Larsen, J. C., and Xu, P.: The Ozone Mapping and Profiler Suite, in:  
354 Earth Science Satellite Remote Sensing, edited by: Qu, J. J., Gao, W., Kafatos, M., Murphy,  
355 R. E., and Salomonson, V. V., Springer, Berlin, 279–296, doi:10.1007/978-3-540-37293-6,  
356 2006.
- 357 Frith, S. M., Kramarova, N. A., Stolarski, R. S., McPeters, R. D., Bhartia, P. K., and Labow, G.  
358 J.: Recent changes in total column ozone based on the SBUV Version 8.6 merged ozone  
359 data set, *J. Geophys. Res.*, 119, 9735–9751, doi:10.1002/2014JD021889, 2014.
- 360 Froidevaux, L., et al., Validation of Aura Microwave Limb Sounder stratospheric and  
361 mesospheric ozone measurements, *J. Geophys. Res.*, 113, D15S20,  
362 doi:10.1029/2007JD008771, 2008.
- 363 Hassler, B., I., Petropavlovskikh, I., Staehelin, J., August, T., Bhartia, P. K., Clerbaux, C.,  
364 Degenstein, D., De Mazière, M., Dinelli, D., Dudhia, A., Dufour, G., Frith, S., Froidevaux,  
365 L., Godin-Beekmann, S., Granville, J., Harris, N., Hoppel, K., Hubert, D., Kasai, Y.,  
366 Kurylo, M., Kyrölä, E., Lambert, J., Levelt, P., McElroy, C., McPeters, R., Munro, R.,  
367 Nakajima, H., Parrish, A., Raspollini, P., Remsberg, E., Rosenlof, K., Rozanov, A., Sano,  
368 T., Sasano, Y., Shiotani, M., Smit, H., Stiller, G., Tamminen, J., Tarasick, D., Urban, J.,  
369 van der A, R., Veeffkind, J., Vigouroux, C., von Clarmann, T., von Savigny, C., Walker, K.,  
370 Weber, M., Wild, J., and Zawodny, J., Past changes in the vertical distribution of ozone –  
371 Part 1: Measurement techniques, uncertainties and availability, *Atmos. Meas. Tech.*, 7,  
372 1395-1427, doi:10.5194/amt-7-1395-1427, 2014.
- 373 Labow, G., McPeters, R., Bhartia, P. K., and Kramarova, N.: A comparison of 40 years of SBUV  
374 measurements of column ozone with data from the Dobson/Brewer network, *J. Geophys.*  
375 *Res.*, 118, 7370–7378, doi:10.1002/jgrd.50503, 2013.
- 376 McPeters, R. D., Kroon, M., Labow, G., Brinksma, E., Balis, D., Petropavlovskikh, I., Veeffkind,  
377 J., Bhartia, P. K., and Levelt, P.: Validation of the Aura Ozone Monitoring Instrument total  
378 column ozone product, *J. Geophys. Res.*, 113, D15S14, doi:10.1029/2007JD008802, 2008.
- 379 McPeters, R. D., Bhartia, P. K., Haffner, D., Labow, G., and Flynn, L.: The version 8.6 SBUV  
380 ozone data record: an overview, *J. Geophys. Res.*, 118, 1–8, doi:10.1002/jgrd.50597, 2013.

381 Seftor, C. J., Jaross, G., Kowitt, M., Haken, M., Li, J., and Flynn, L., Postlaunch performance of  
382 the Suomi National Polar orbiting Partnership Ozone Mapping and Profiler Suite (OMPS)  
383 nadir sensors, *J. Geophys. Res. Atmos.*, 119, 4413–4428, doi:10.1002/2013JD020472,  
384 2014.

385 Witte, J. C., et al., First reprocessing of Southern Hemisphere ADditional OZonesondes  
386 (SHADOZ) profile records (1998-2015): 1. Methodology and evaluation, *J. Geophys. Res.*  
387 *Atmos.*, 122, 6611-6636, doi:10.1002/2016JD026403, 2016.

388 Ziemke, J. R., et al.: A global climatology of tropospheric and stratospheric ozone derived from  
389 Aura OMI and MLS measurements *Atmos. Chem. Phys.*, 11 (17): 9237-9251  
390 (10.5194/acp-11-9237-2011), 2011.

391 Ziemke, J. R., et al.: Assessment and applications of NASA ozone data products derived from  
392 Aura OMI/MLS satellite measurements in context of the GMI chemical transport model, *J.*  
393 *Geophys. Res. Atmos.*, 119 (9): 5671-5699 (10.1002/2013JD020914), 2014.

394

395 **Figure Captions**

396

397 Figure 1. Each orbit of NM data measures a swath of total column ozone. 35 individual ozone  
398 measurements (see example near equator) are made for each scan line.

399

400 Figure 2. OMPS ozone will be compared with MOD (merged ozone data) ozone created by  
401 merging data from recent SBUV/2 instruments. Monthly average ozone for 60°S-60°N is plotted.

402

403 Figure 3. A comparison of OMPS NM ozone (in black) and NOAA 19 SBUV (in blue) with  
404 average ozone from an ensemble of 52 northern hemisphere Dobson and Brewer stations. A  
405 linear fit to the NM data is also shown. Weekly mean percent difference of satellite ozone minus  
406 ground-based ozone is plotted.

407

408 Figure 4. For average ozone in the 60°S - 60°N latitude zone (lower panel), the average bias of  
409 NM ozone relative to MOD (upper panel) was reduced from 0.99% in version 1 to -0.20% in the  
410 version 2 processing.

411

412 Figure 5. A similar plot for the OMPS nadir profiler shows that the large bias in the released vsn  
413 1 data is reduced in the vsn 2 processing.

414

415 Figure 6. In version 2 the four year average of March ozone latitude dependence (2013-2016) is  
416 shown in the lower panel for the mapper (dashed blue curve) and for the profiler (solid red  
417 curve). Percent differences from MOD are shown in the upper panel.

418

419 Figure 7. An average of ozone sonde data from Hilo Hawaii is compared with OMPS NP vsn 2  
420 ozone profiles for coincident days, with percent difference plotted in the right panel. The NP  
421 profile integrates to 274.1 DU, while the sonde profile integrates to 272.5 DU when a  
422 climatological stratospheric amount is added.

423

424 Figure 8. The NP ozone anomaly, the difference from NOAA 19 ozone, for mid and low  
425 latitudes is shown as a function of time for total column ozone, the lower stratosphere, and the  
426 upper stratosphere. Ozone from the version 1 processing (in red) and the version 2 processing (in  
427 green) are shown.

428

429 Figure 9. OMPS NP v2 June zonal average ozone profiles (2012-2016) compared with NOAA  
430 19 SBUV/2 profiles, MLS profiles, and profiles from the OMPS LP. OMPS NP vsn 2 percent  
431 differences from N19, MLS, and LP are plotted on the right.

432

433 Figure 10. The time dependence of the v2.0 ozone anomaly relative to NOAA 19 shown for low  
434 to mid latitudes.

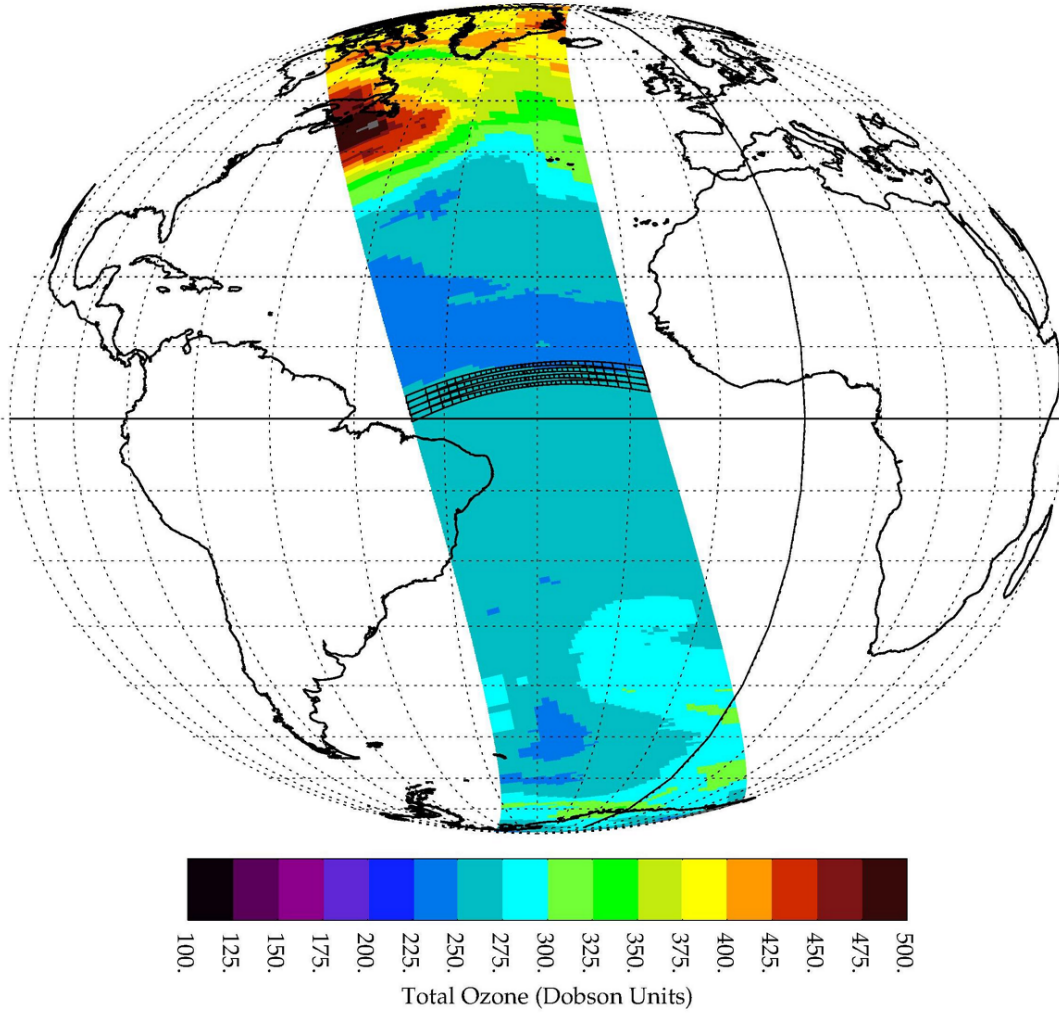
435

436 Figure 11. The time dependence of the v2.0 ozone anomaly relative to NOAA 19 shown for high  
437 latitudes.

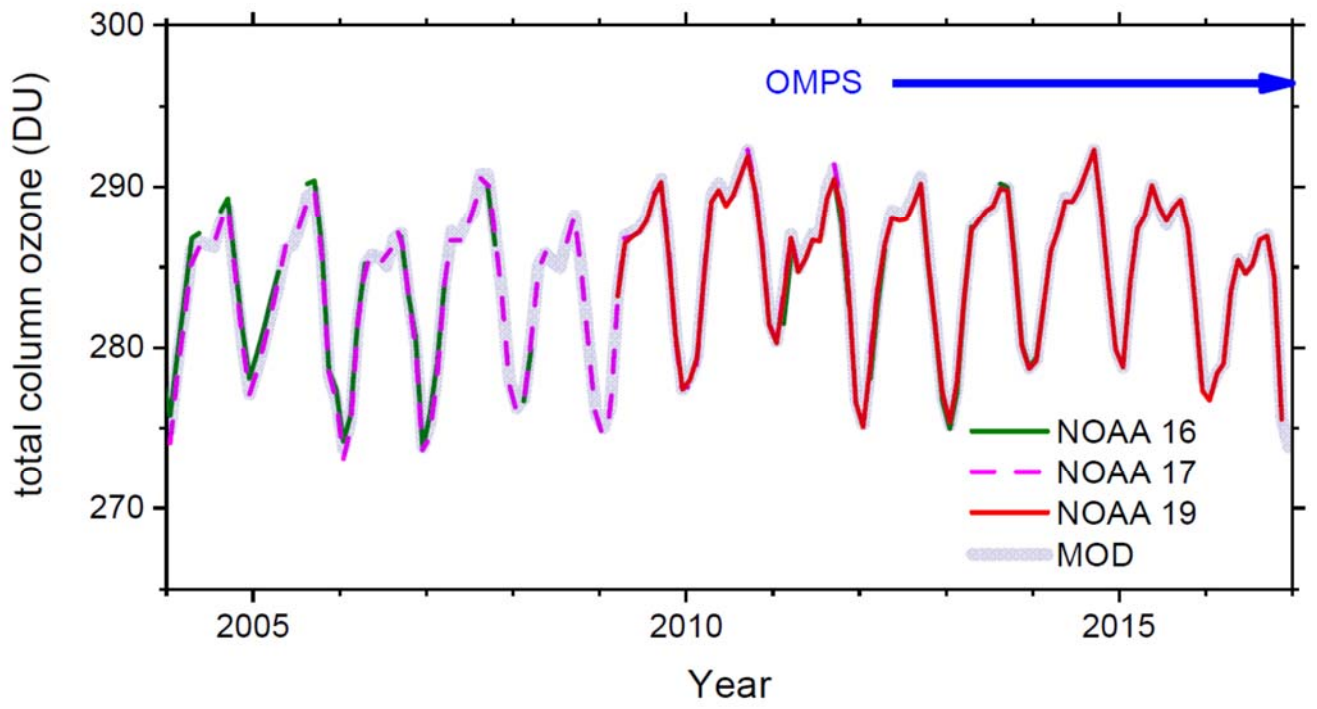
438  
439 Figure 12. The time series of tropospheric ozone shown for four locations. Tropospheric ozone  
440 derived by subtracting OMPS LP stratospheric ozone from NM total column ozone is shown in  
441 the blue solid curve, while tropospheric ozone derived by subtracting MLS stratospheric ozone  
442 from OMI total column ozone is shown in the dashed red curve.

443

March 23, 2013

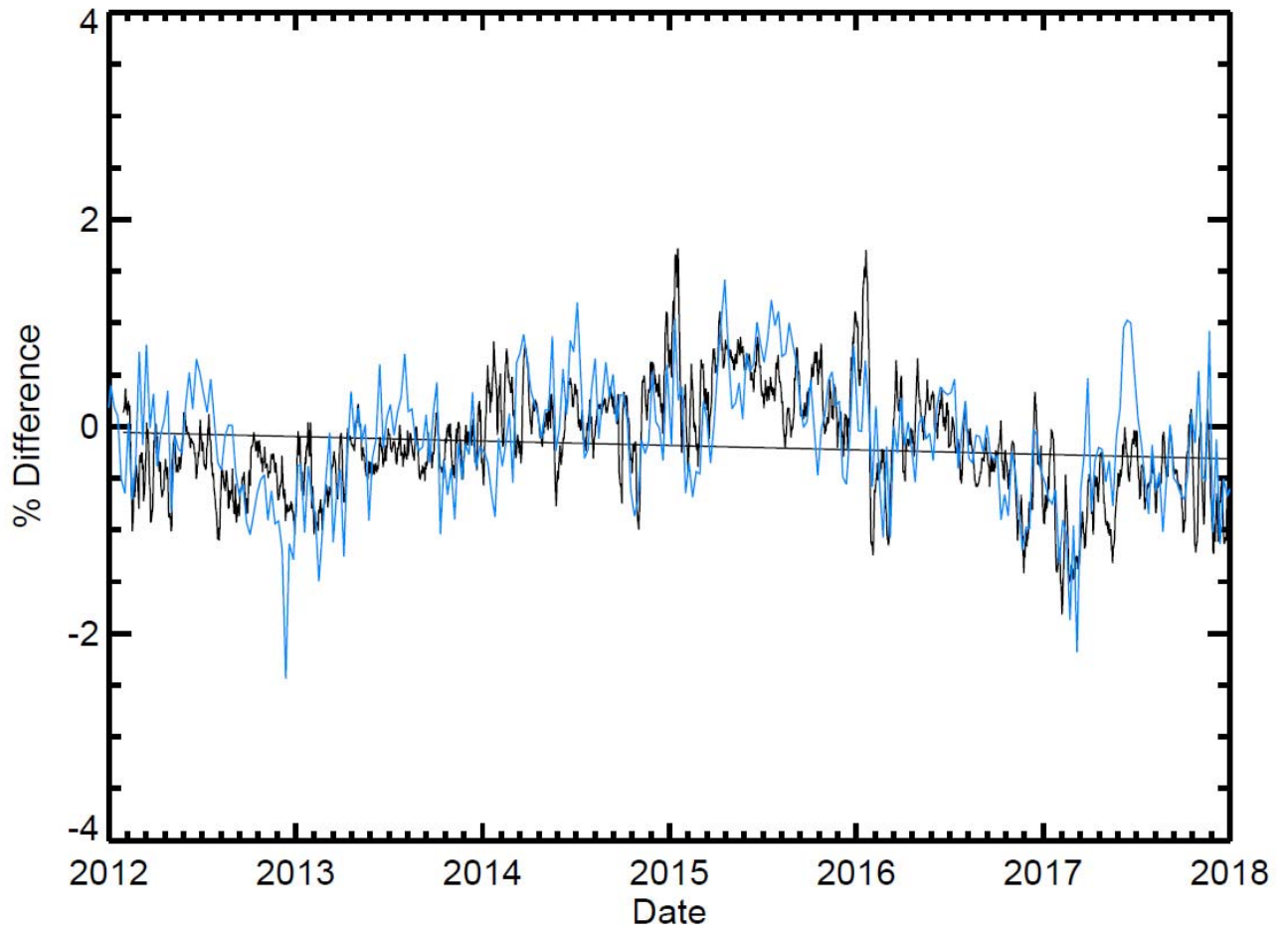


471 Figure 1



472  
473

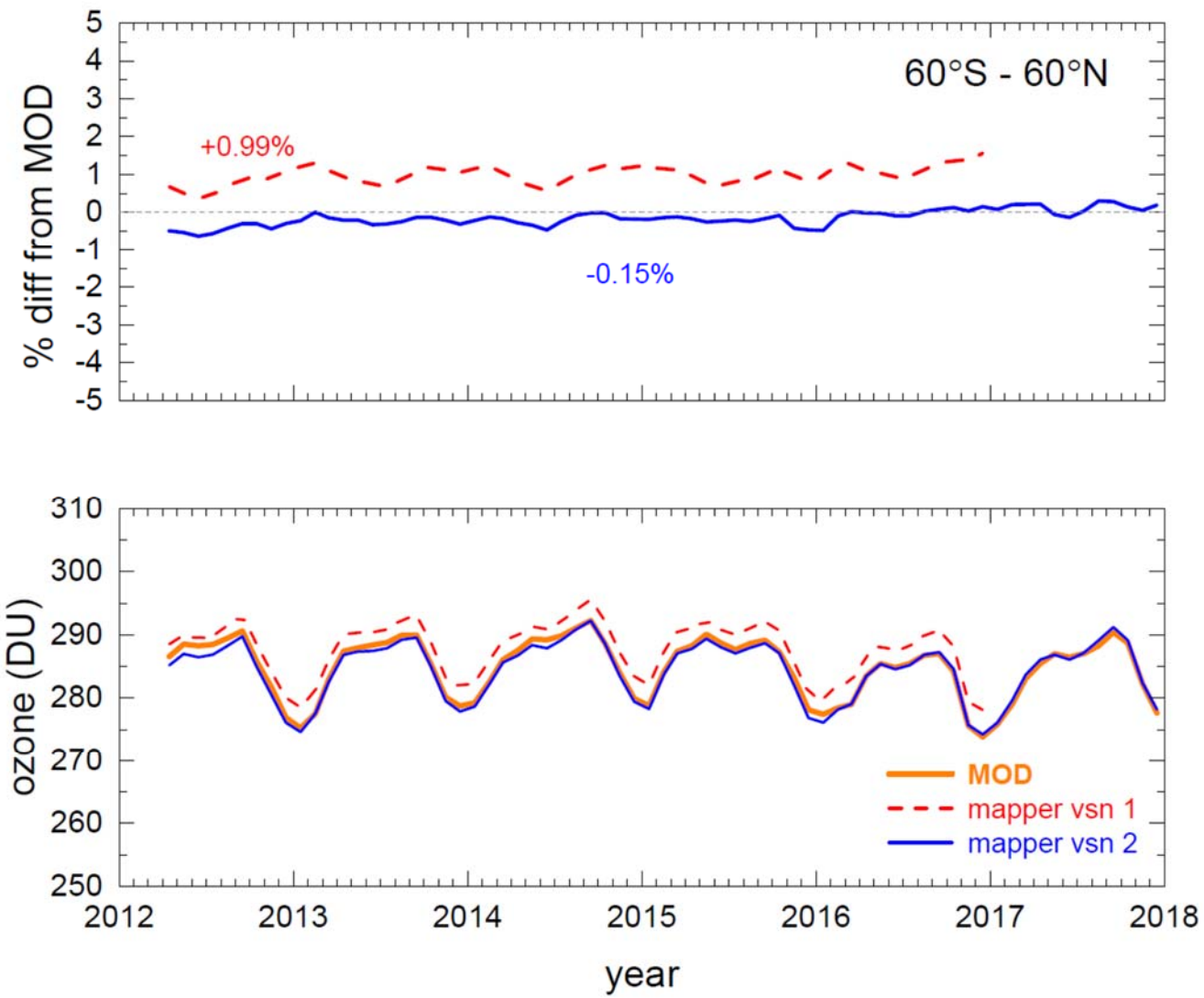
Figure 2



474  
475

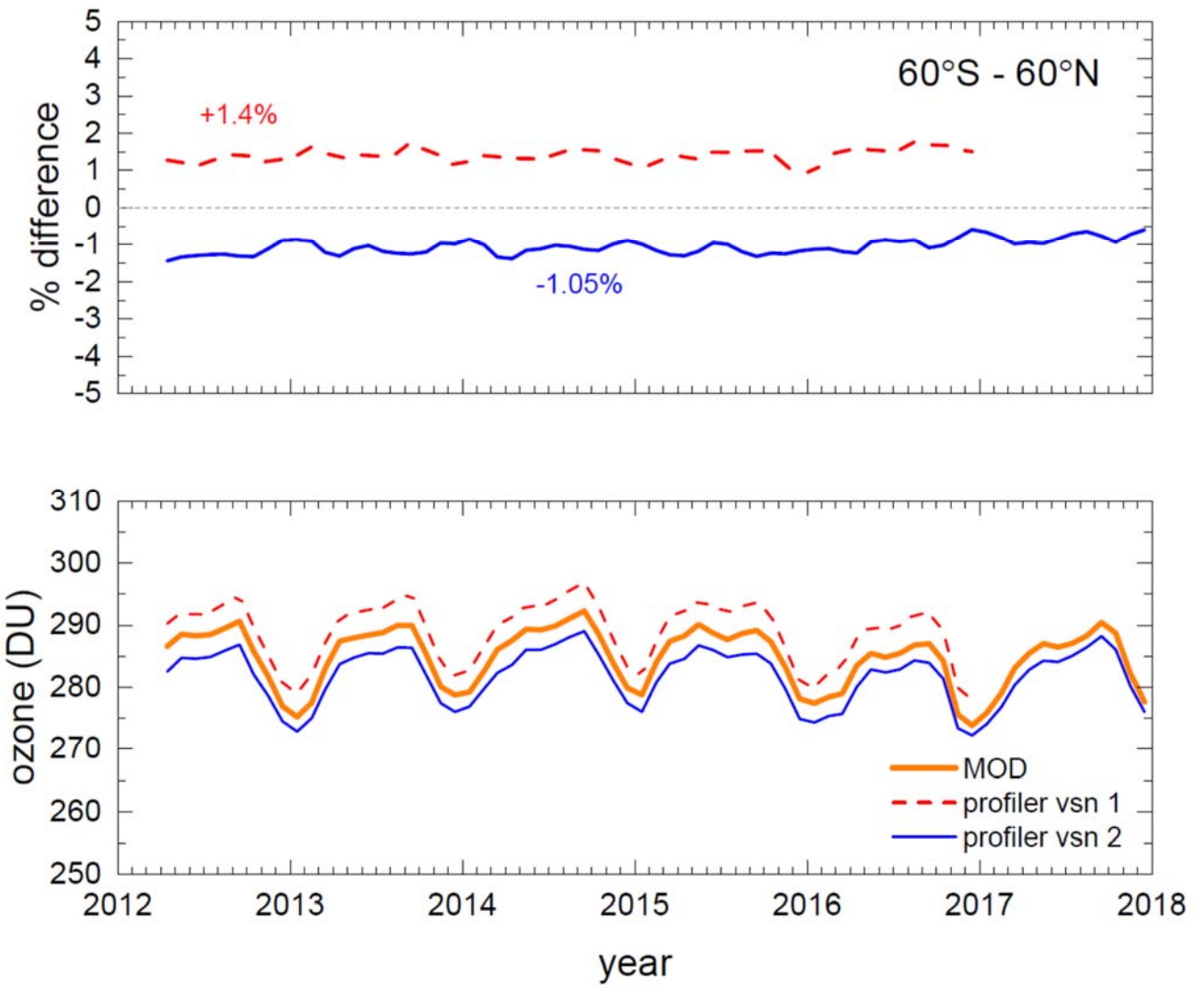
Figure 3





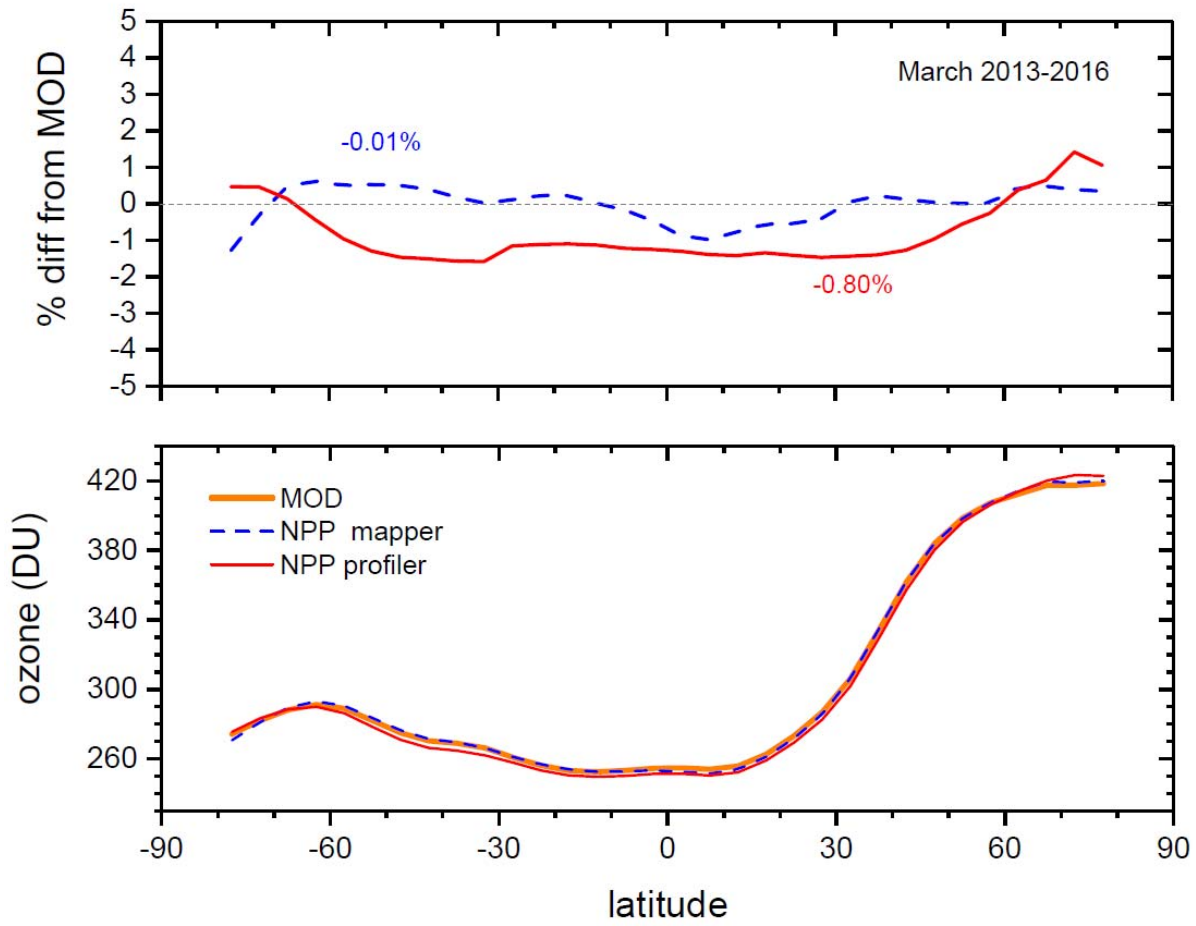
476  
477  
478

Figure 4



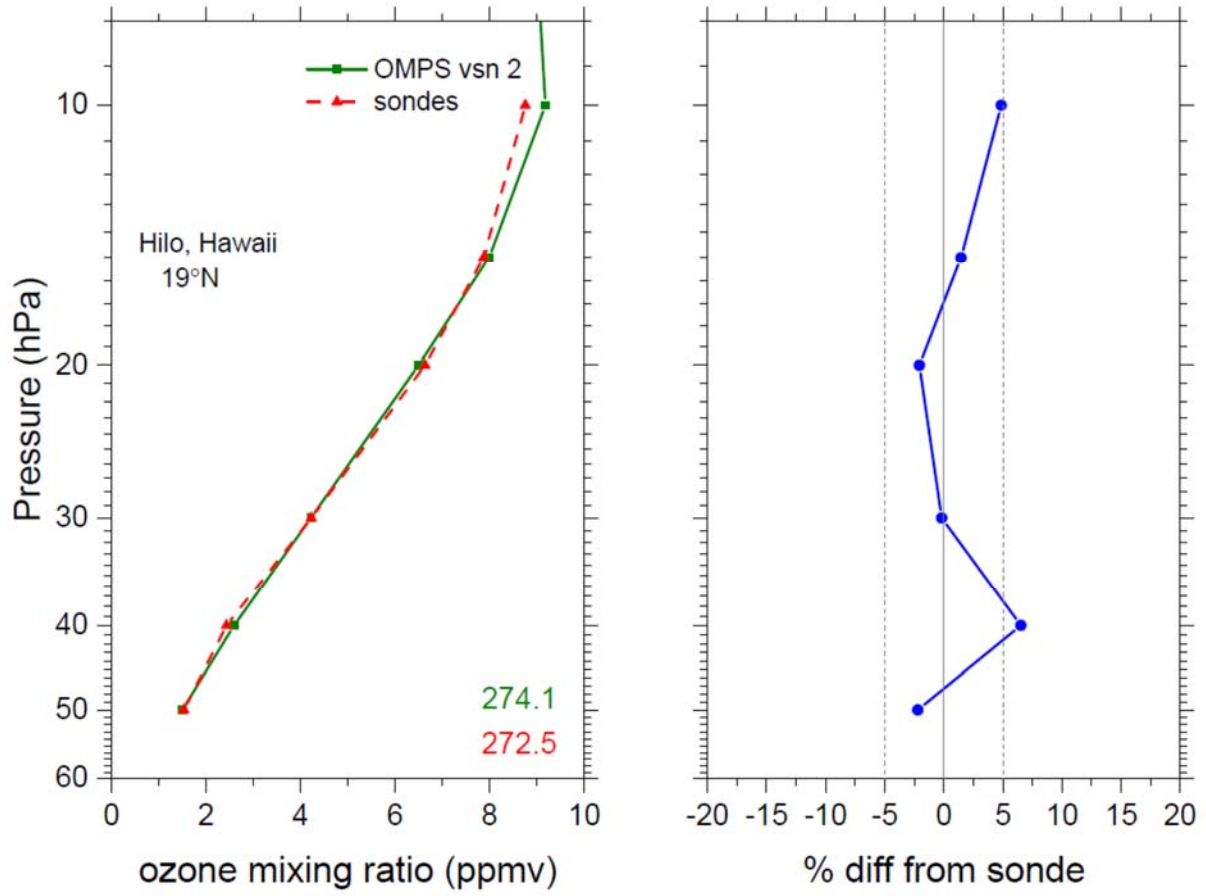
479  
 480  
 481

Figure 5



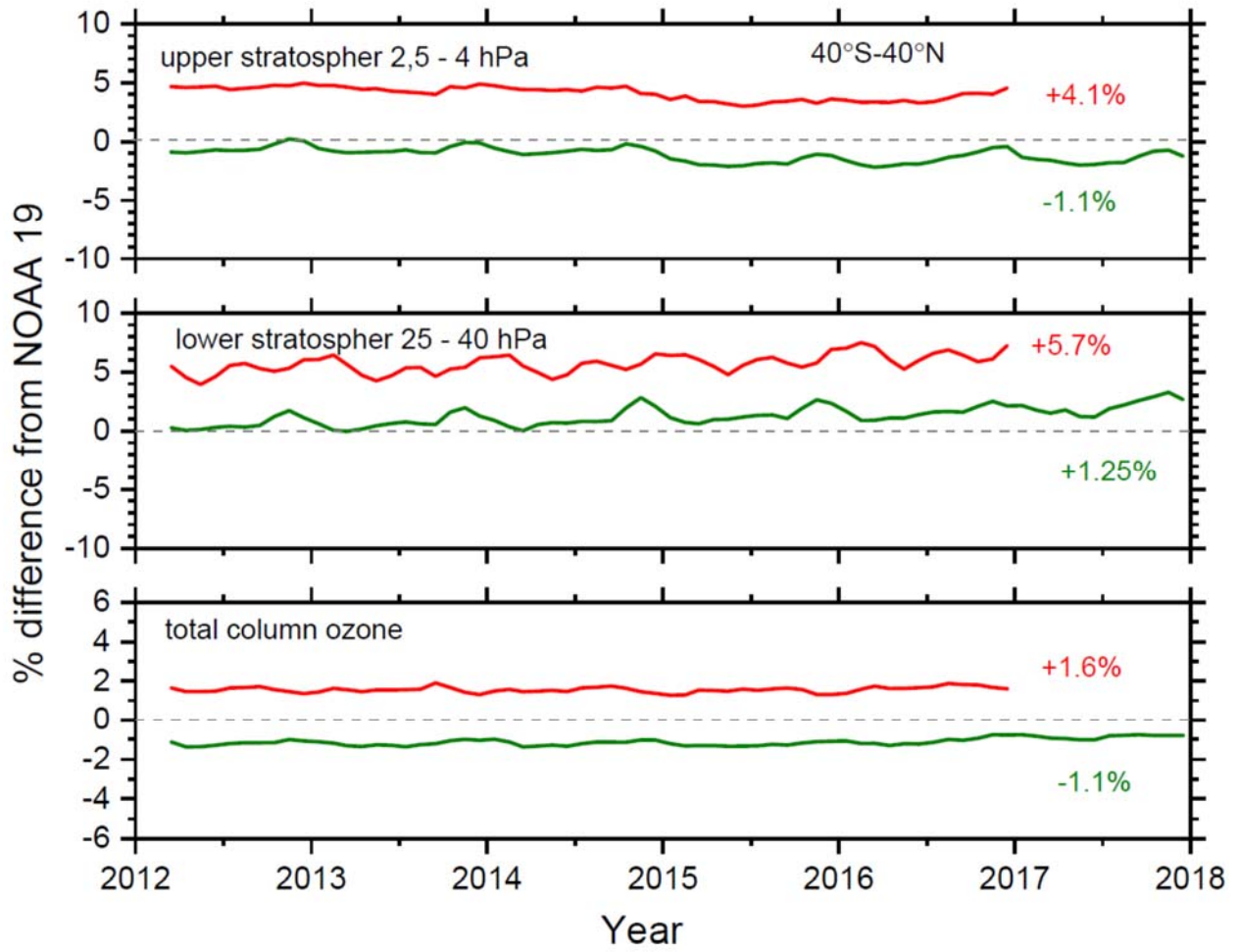
482 Figure 6  
 483

### Hilo sondes - annual average 2016



484  
485

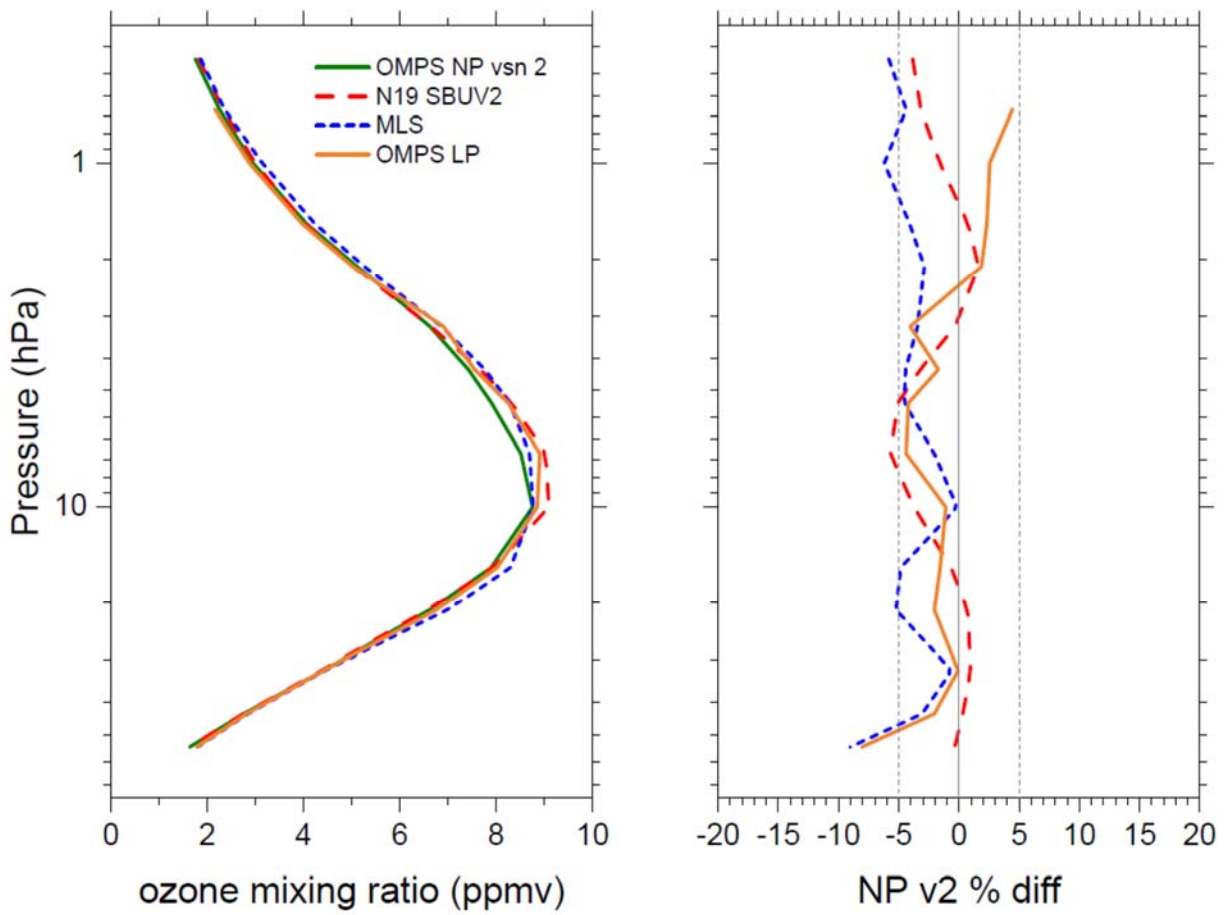
Figure 7



486  
487

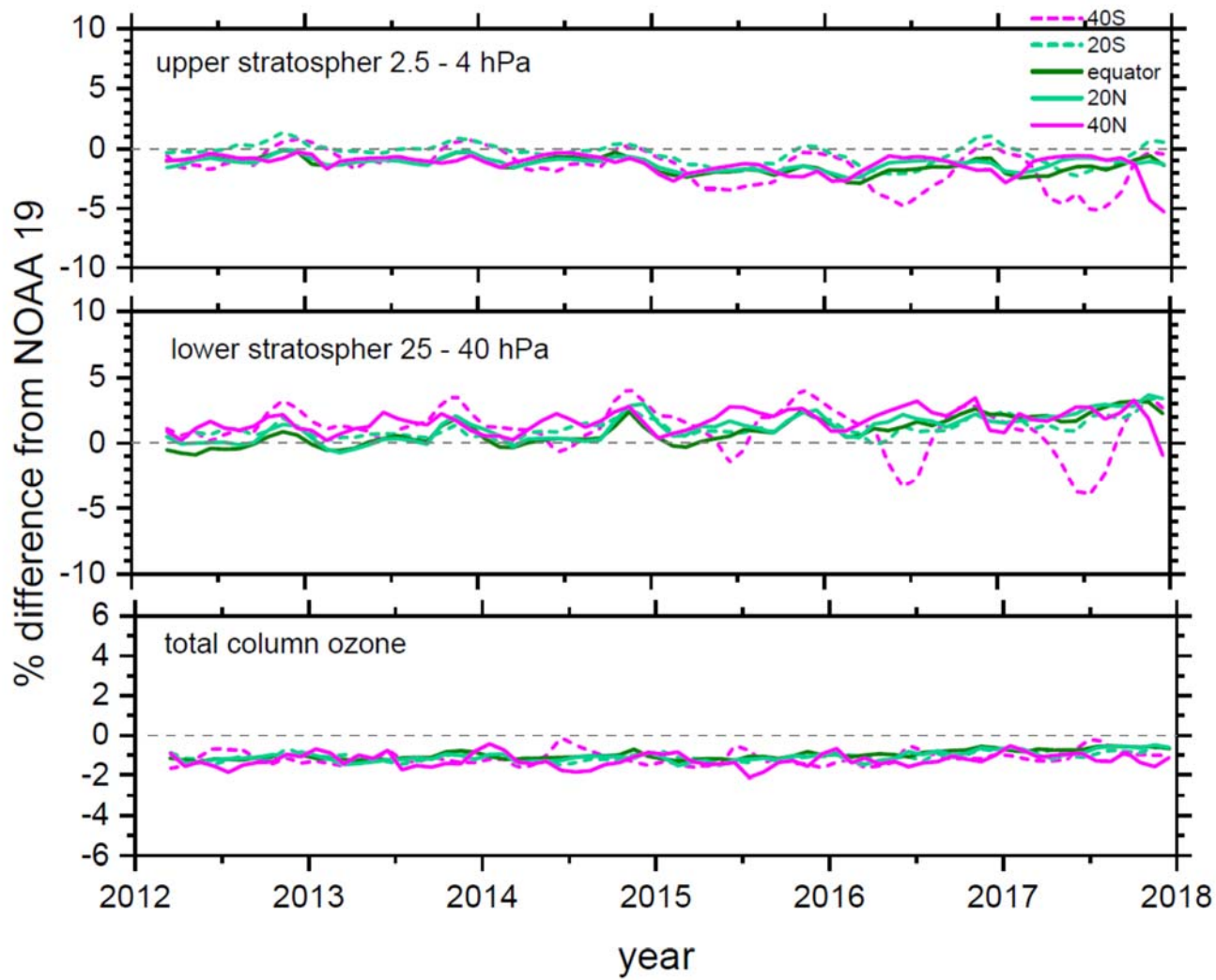
Figure 8

June average 2012-2016 40°S - 40°N



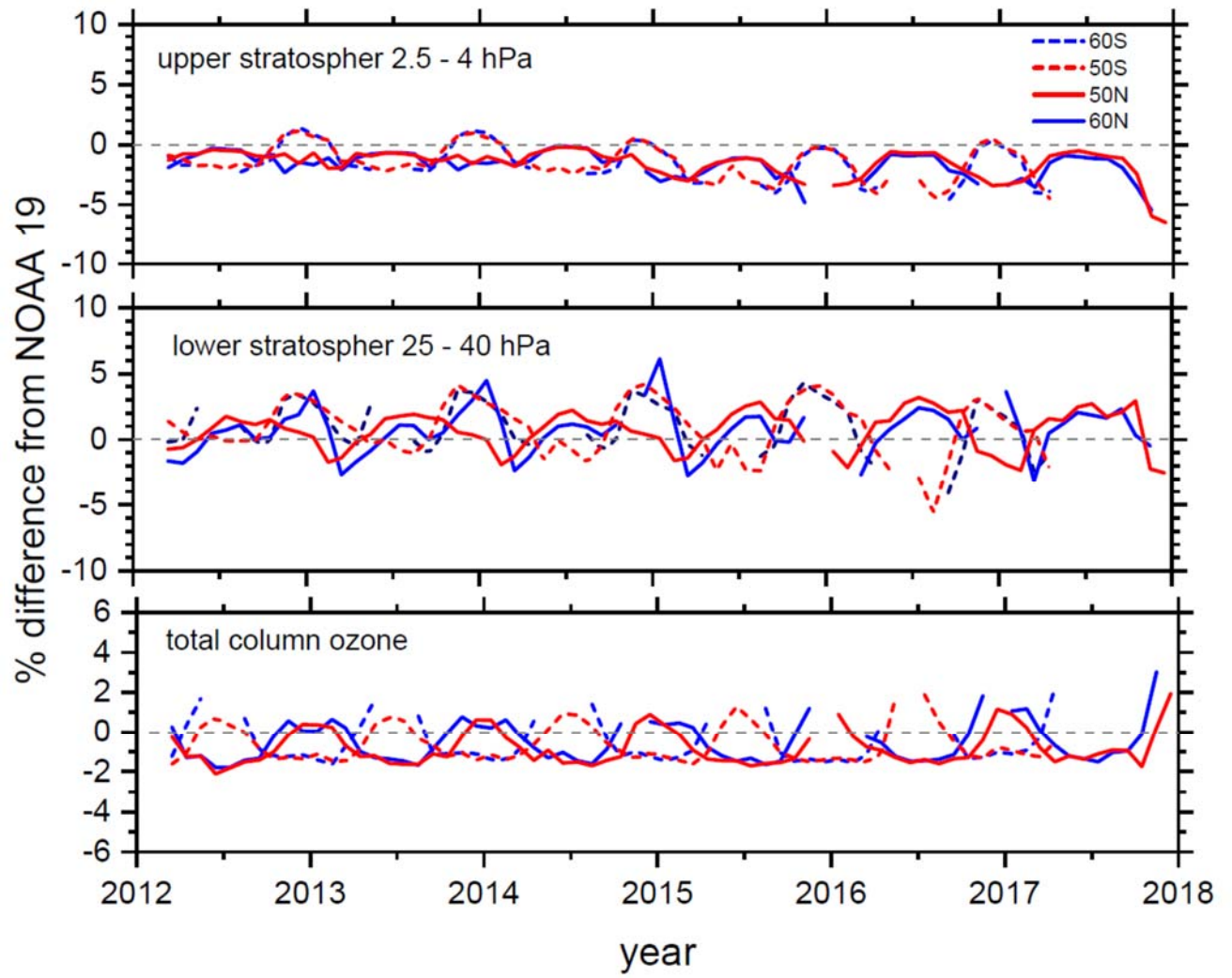
488  
489

Figure 9



490  
491

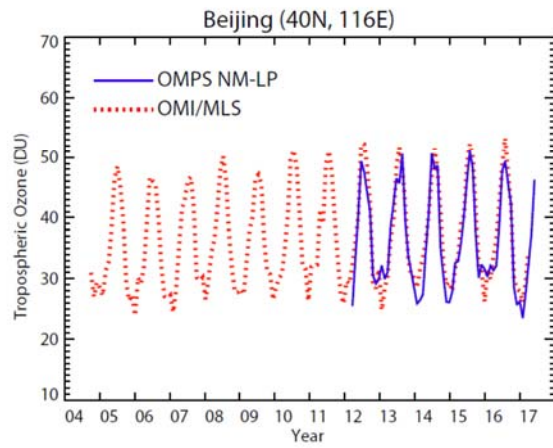
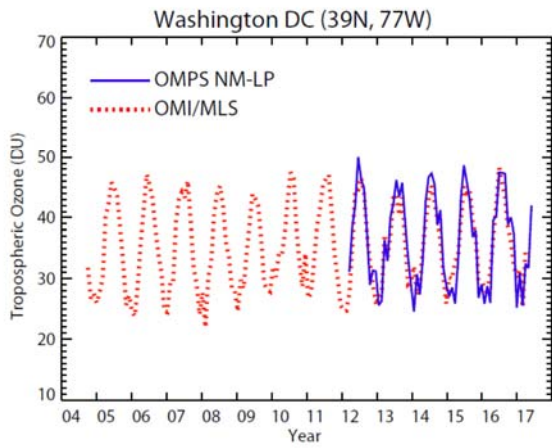
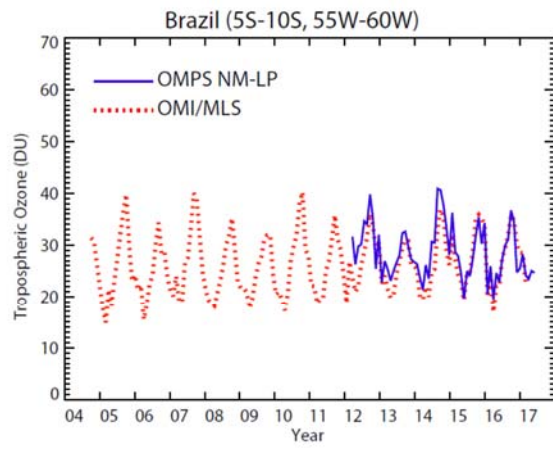
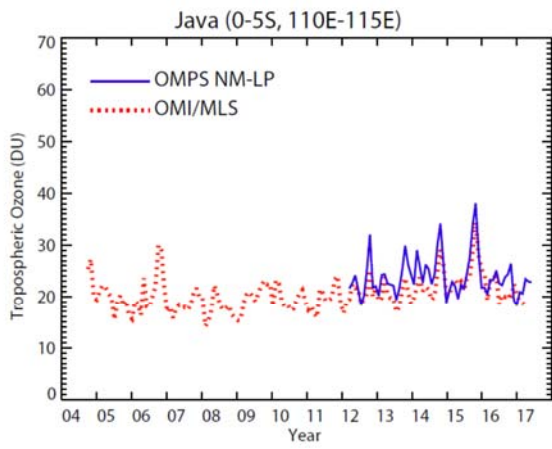
Figure 10



492  
493

Figure 11





494  
495  
496

Figure 12